Microporous and Mesoporous Materials 143 (2011) 125–131

Contents lists available at ScienceDirect

Microporous and Mesoporous Materials

journal homepage: www.elsevier.com/locate/micromeso

Molecular dynamics investigation of the self-diffusion of binary mixture diffusion in the metal-organic framework Zn(tbip) accounting for framework flexibility

K. Seehamart [a], C. Chmelik [b], R. Krishna [c], S. Fritzsche [a,*]

[a] University of Leipzig, Faculty of Physics and Geosciences, Institute of Theoretical Physics, Postfach 100920, 04009 Leipzig, Germany
[b] University of Leipzig, Faculty of Physics and Geosciences, Institute of Experimental Physics I, Linnéstraße 5, D-04103 Leipzig, Germany
[c] Van't Hoff Institute for Molecular Sciences, University of Amsterdam, The Netherlands

ARTICLE INFO

Article history:
Received 12 November 2010
Received in revised form 9 February 2011
Accepted 13 February 2011
Available online 24 February 2011

Keywords:
Self-diffusivity
Molecular dynamics
Lattice flexibility
Metal-organic frameworks
Mixture

ABSTRACT

The self-diffusion of three equimolar mixtures in the metal-organic framework Zn(tbip) has been investigated by molecular dynamics simulations. The simulations take due account of lattice flexibility. The diffusional characteristics are discussed in relation to molecule properties and lattice geometry. The results show that Zn(tbip) may be a useful material for separating methane/ethane and CO_2/ethane mixtures at low concentrations, and CO_2/methanol mixtures at high concentrations.

1. Introduction

Molecular dynamics (MD) simulation is a powerful technique widely used to obtain detailed information on structure and dynamics of the guest molecules in microporous materials such as zeolites and MOFs [1]. However, most of the simulations are often performed with the assumption that the framework is rigid. This assumption is a reasonable approximation for zeolites [2,3]. The situation with MOFs is somewhat different. Using rigid and flexible framework, the loading dependence of the self-diffusion coefficient of ethane in metal-organic framework (MOF) of type Zn(tbip) shows surprising effects arising from the lattice flexibility [4,5] in comparison to the rigid model. Lattice flexibility increases the self-diffusivities and also leads to a maximum at intermediate loadings. In contrast, for IRMOF-1 it had been shown that the self-diffusivities of several guest molecules were not much influenced by the lattice flexibility [6].

In the present paper the investigations for guest molecules in Zn(tbip) have been extended to methane, CO_2, and methanol, which are different in molecular sizes and charges. The surprising effect (maximum) found for ethane does not appear for methane, CO_2 and even methanol, but is obviously connected with the special properties of the ethane molecules. Additionally, the diffusion of mixtures of those guest molecules in Zn(tbip) have been examined as well because the curvature of the channel walls lets us expect that molecules of different sizes will show different diffusive behavior making Zn(tbip) possibly useful for separation purposes. These systems are investigated in detail in this study.

2. Model and simulations

In this study, CO_2 was modeled as a three Lennard–Jones sites model with charges centered at each atom ($q_c = 0.6512e$ and $q_o = -0.3256e$) with bonds length C–O of 1.16 Å, and the interaction parameters were taken from the work of Krishna et al. [7,8] as listed in Table 1. Using this model, they performed MD simulations to study the CO_2 and CO_2/methane mixture in CHA and DDR zeolite at 300 K, and reported the CO_2 self-diffusivity in the range of $0.1-5.0 \times 10^{-9}$ m^2 s^{-1}.

Methane was modeled by the united atom model, and ethane was modeled as two united atoms with a fixed bond length of 1.53 Å which is the same model used in our previous work [4,5]. The intermolecular potential parameters of methane and ethane were taken from the transferable potentials for phase equilibria (TraPPE) model [9], also given in Table 1. Using this model, Krishna and van Baten [10] reported the self-diffusivity of methane in Zn(tbip) (rigid framework) in the range of $10^{-11}-10^{-8}$ m^2 s^{-1}. Skoulidas and Sholl [11] reported the values in the range of $2-3 \times 10^{-8}$ m^2 s^{-1} for methane in IRMOF-1 at room temperature. Garberoglio and Vallauri [12] reported values in the range of $7.7-22.5 \times 10^{-8}$ m^2 s^{-1} for methane in 2D–COFs at 289 K.

* Corresponding author.
E-mail address: siegfried.fritzsche@uni-leipzig.de (S. Fritzsche).

1387-1811/$ - see front matter © 2011 Elsevier Inc. All rights reserved.
doi:10.1016/j.micromeso.2011.02.018

Table 1
LJ and Coulomb potential parameters of guest molecules used in this study.

Adsorbate	Site–site	ϵ (kJ/mol)	σ (Å)	Charge (e)	Bond (Å)
CH_4	CH_4	1.2305	3.730	0	–
C_2H_6	CH_3	0.8148	3.750	0	1.53; (C—C)
CO_2	C	0.2339	2.757	0.6512	1.16; (C=O)
	O	0.6694	3.033	−0.3256	–
CH_3OH	C	0.6696	3.475	−0.0930	1.105; (C—H_C)
	H_C	0.1592	2.450	0.100	1.420; (C—O)
	O	0.9533	2.860	−0.432	0.945; (H_O—O)
	H_O	–	–	0.225	–

Table 2
Bonded interaction parameters for the flexible methanol molecule used in this study.

$i-j$	k_r (kJ/mol · Å^2)		r_0 (Å)	
Bond stretching				
C—H_C	2852.11		1.105	
C—O	3215.86		1.420	
H_O—O	3451.92		0.945	
Angle bending				
$i-j-k$	k_θ (kJ/mol · rad^2)		θ_0 (degree)	
C—O—H_O	540.318		108.32	
H_C—C—O	530.669		106.90	
H_C—C—H_C	424.535		108.38	
$i-j-k-l$	k_ϕ (kJ/mol)	ϕ_0 (degree)	α	m
Torsion				
$H_C-C-O-H_O$	0.7352	180.0	1.0	3

However, larger values of $\approx 1.7 \times 10^{-7}$ m^2 s^{-1} have been found experimentally by Stallmach et al. [13] for methane in IRMOF-1.

The flexible methanol molecule was modeled by bonding, bond-bending, and torsion potentials, as given in Eq. (1). Non-bonded interactions acting between methanol molecules were described by the Coulomb and Lennard–Jones potentials, as expressed by Eq. (2). Both bonded and non-bonded potential parameters were taken from the work of Plant et al. [14] for methanol diffusion in the NaY zeolite as listed in Tables 1 and 2. The validity of these force field parameters was confirmed by an agreement of the diffusion coefficient of methanol obtained in the liquid phase by simulation to be 1.365×10^{-9} m^2 s^{-1} at an ambient temperature with the corresponding experimental results of 1.3×10^{-9} m^2 s^{-1} [15]. In addition, Nanok et al. [16] also used these parameters to study the methanol in NaX zelozite. Their adsorption structure results agree well with the experimental IR spectroscopic data, and the self-diffusivity values are in the range of 1.0—1.2 $\times 10^{-9}$ m^2 s^{-1}

$$U_{\text{methanol}} = \frac{1}{2}k_r(r-r_0)^2 + \frac{1}{2}k_\theta(\theta-\theta_0)^2 + k_\phi[1+\alpha\cos(m\phi-\phi_0)]. \quad (1)$$

The force field parameters for the flexible Zn(tbip) framework were taken from our previous work [4,5], and they are described in detail in the supplementary material to [4]. To complete them, the non-bonded interactions between the guest–guest as well as the guest-Zn(tbip) molecules were modeled by the LJ and Coulombic potential given by

$$U(r_{ij}) = 4\epsilon_{ij}\left[\left(\frac{\sigma_{ij}}{r_{ij}}\right)^{12} - \left(\frac{\sigma_{ij}}{r_{ij}}\right)^{6}\right] + \frac{1}{4\pi\epsilon_0}\frac{q_i q_j}{r_{ij}}, \quad (2)$$

where ϵ_{ij} is the LJ well-depth, σ_{ij} is the LJ diameter, and r_{ij} is the distance between two interacting atoms i and j. The Lorenz–Berthelot mixing rules were used to obtain the cross potentials $\sigma_{ij} = (\sigma_i + \sigma_j)/2$ and $\epsilon_{ij} = \sqrt{\epsilon_i \epsilon_j}$.

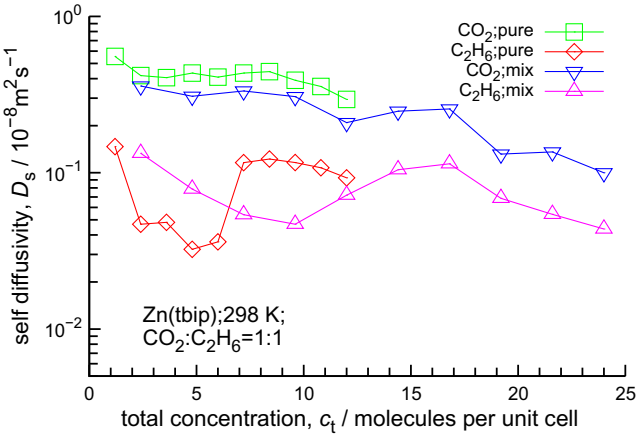

Fig. 1. The self-diffusivities of CO_2 and C_2H_6 both for pure components and 1:1 mixture in Zn(tbip) flexible framework.

Table 3
Self-diffusivities of equimolar mixtures of CO_2/ethane, methane/ethane, CO_2/methanol, and their pure components in Zn(tbip) flexible framework for the range of studied concentrations.

Asorbates	Components	D_s (10^{-8} m^2 s^{-1})
CH_4	Pure	0.58–1.60
	CH_4/C_2H_6	0.09–0.95
CO_2	Pure	0.30-0.56
	CO_2/CH_3OH	0.11–0.39
	CO_2/C_2H_6	0.09–0.36
CH_3OH	Pure	0.09–0.24
	CO_2/CH_3OH	0.03–0.30
C_2H_6	Pure	0.09–0.15
	CH_4/C_2H_6	0.04–0.15
	CO_2/C_2H_6	0.04–0.14

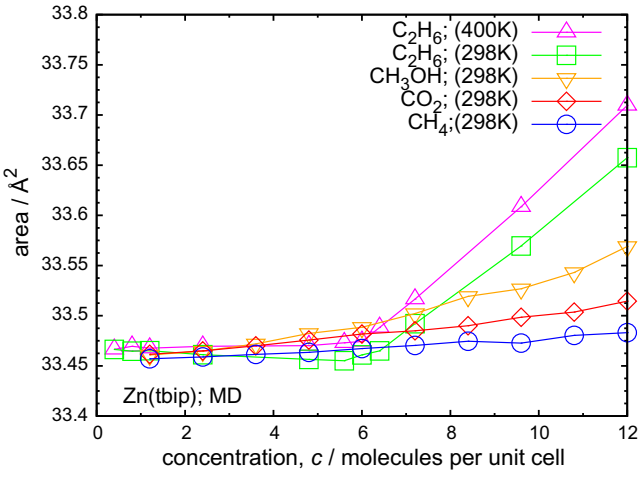

Fig. 2. The cross section area of the window as a function of concentration for pure component of methane, CO_2, methanol and ethane in Zn(tbip) flexible framework. The cross section areas are calculated in the NVT ensemble.

Our molecular dynamics simulations of methane/ethane, CO_2/ethane and CO_2/methanol mixture in Zn(tbip) have been carried out, like the earlier simulations of single component ethane diffusion in Zn(tbip) [4,5] using the DL_POLY simulation package [17] on a Linux workstation cluster. The simulation box has the dimensions of 28.863 × 49.992 × 39.855 Å. This contains five unit cells of Zn(tbip) and comprises of 5220 framework atoms. Periodic

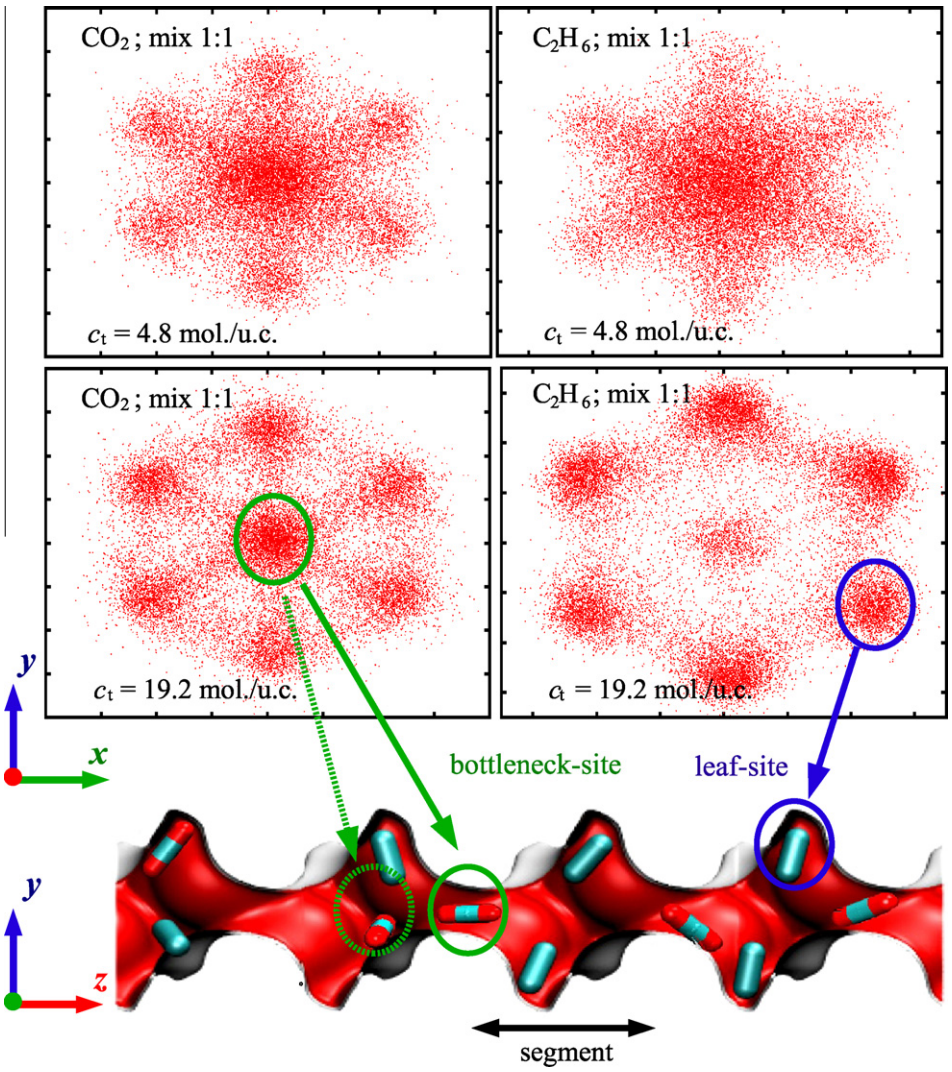

Fig. 3. The center-of-mass distribution of a CO_2 and ethane molecule projected into the *xy* plane tracked every 0.5 ps during a simulation period of 10 ns for CO_2:ethane = 1:1 mixture in Zn(tbip) flexible framework.

boundary conditions have been applied to all three directions. The long-range electrostatic interactions between the Zn(tbip) framework atoms have been computed using the Ewald summation technique, and the short-range van der Waals interactions between framework atoms and between framework and guest molecules have been computed up to a cutoff radius of 12 Å. The MD simulations were performed in the NVE ensemble at the temperature of 298 K. The equations of motion were integrated by using the velocity Verlet algorithm with a time step of 1 fs. In each loading, every channel of Zn(tbip) is loaded with an equal number of guest molecules. The starting configuration was used as input for 500 ps equilibration period at 298 K. After that, velocity rescaling was switched off and an equilibration of 500 ps was performed to ensure that there were no further drifts. Then, the production runs have been conducted for 10 ns. During the production runs, the coordinates have been stored every 100 fs for further analysis.

By using Einstein's relation [18], Eq. (3), we calculated one-dimensional self-diffusion coefficients for each kind of molecule pure and in mixture from the slope of the mean-squared displacement (MSD) as function of time

$$D_{s,i} = \frac{1}{2N_i} \lim_{\Delta t \to \infty} \frac{1}{\Delta t} \left\langle \sum_{l=1}^{N_i} \left[z_{l,i}(t + \Delta t) - z_{l,i}(t) \right]^2 \right\rangle \quad (3)$$

where $D_{s,i}$ is the center of mass self-diffusivity of molecules of species i, N_i is the number of molecules of species i, and $z_{l,i}(t)$ is the position of molecule l of species i at any time t.

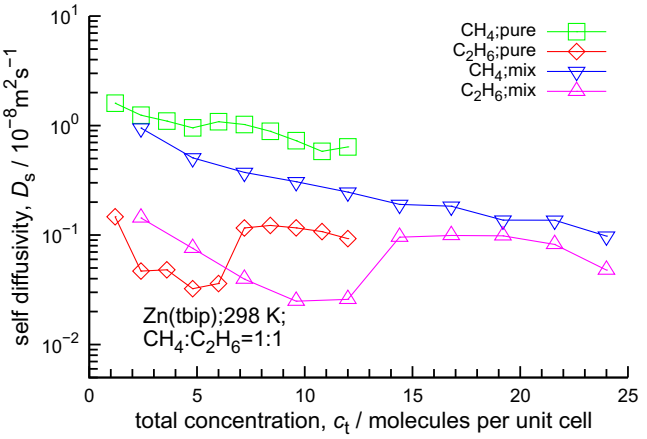

Fig. 4. The self-diffusivities of methane and ethane both for pure components and 1:1 mixture in Zn(tbip) flexible framework.

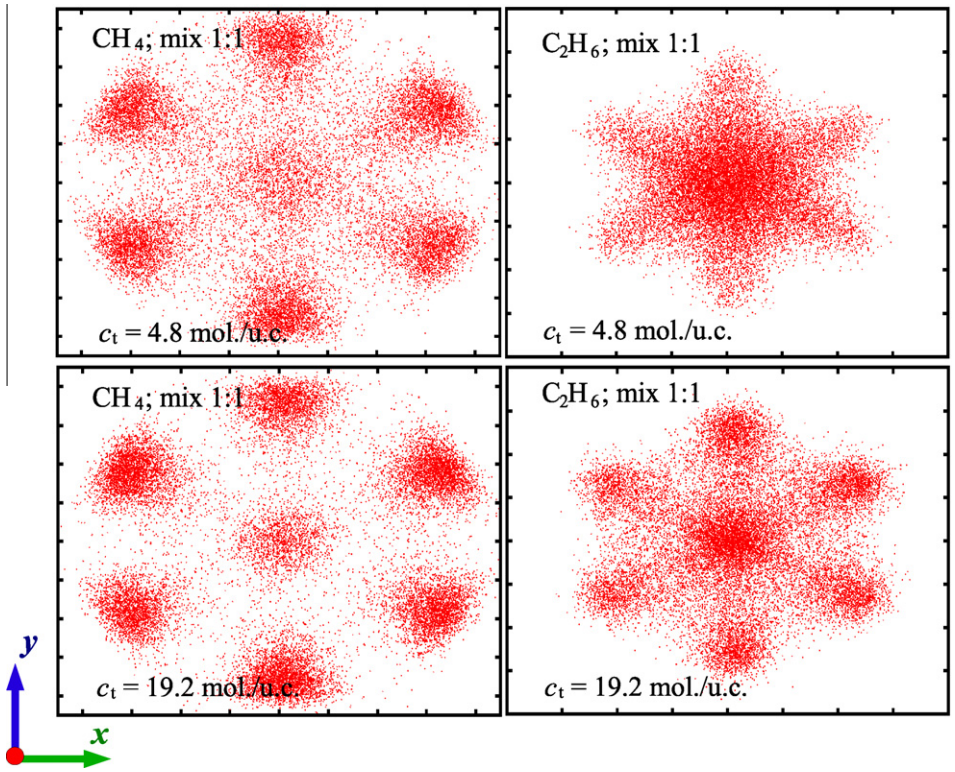

Fig. 5. The center-of-mass distribution of a methane and ethane molecule projected into the *xy* plane tracked every 0.5 ps during a simulation period of 10 ns for methane:ethane = 1:1 mixture in Zn(tbip) flexible framework.

From the self-diffusivities the diffusion selectivities have been further examined. The diffusion selectivity [8]; $\alpha_{A,B}^{diff}$, is defined as the ratio of the self-diffusivities of molecules of species A and of species B in a binary mixture, so that $\alpha_{A,B}^{diff}$ is given by

$$\alpha_{A,B}^{diff} = \frac{D_{s,A}}{D_{s,B}} \tag{4}$$

where $D_{s,A}$ is the self-diffusivity of molecules of species A, and $D_{s,B}$ is the self-diffusivity of molecules of species B. Values of $\alpha_{A,B}^{diff}$ greater than unity imply that A is diffusing faster than B.

3. Results

The results showed that the maximum in the self-diffusivity of ethane as a function of loading that was shown to be present only in the flexible lattice appears also in the mixture. The reasons for this maximum have been explained in [5]. For the other diffusants examined in this paper pure and in mixture the loading dependence of the self diffusivity is a monotonic one. This is the common form of loading-dependence of self-diffusivities which arises from the mutual steric hindrance of diffusing molecules and was observed for many other adsorbate molecules in many MOFs [10,19–21].

In the mixtures the slower molecule always slowed down the mobility of the faster one and the faster one somewhat drags the slowly diffusing one.

3.1. CO_2/ethane mixture in Zn(tbip)

Self-diffusivities of equimolar mixtures of CO_2/ethane and of pure components in Zn(tbip) flexible framework as function of the total concentration are shown in Fig. 1. The data are also given in Table 3 for completenes. Both, pure and in mixture, CO_2 self-diffusivity is found to be higher than that of C_2H_6 over the entire range of total concentration, c_t.

Fig. 3 shows the center-of-mass density distribution of the CO_2/ethane mixture in Zn(tbip) at different total loading. At low loading ethane molecules preferably adsorb near the center of the channel and the middle of the segment. CO_2 on the one hand has a dipole moment and on the other hand is more slender can diffuse around the whole segment and can also diffuse through the window into the adjacent segments. Because of this the self-diffusivity of CO_2 is higher than that of ethane. At high total concentrations, the mutual repulsion between molecules in the same segment causes the ethane molecule to be significantly adsorbed within the leaf

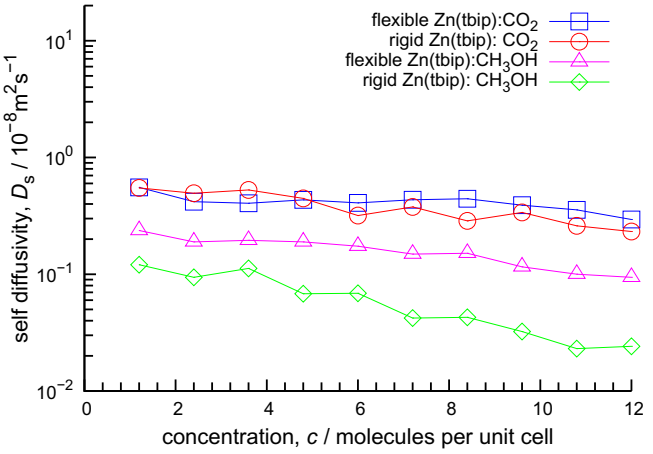

Fig. 6. The self-diffusivities of CO_2 and methanol for pure components in rigid and flexible Zn(tbip) framework.

positions. By contrast, however, CO_2 is still fastly diffusing in the same segment and hopping to the adjacent segments. In consequence, the self–diffusivity of CO_2 is still higher than that of ethane.

3.2. Methane/ethane mixture in Zn(tbip)

In Fig. 4 the self-diffusivities of equimolar mixtures of methane/ethane and pure components in Zn(tbip) with flexible framework as a function of the total concentration are shown. Methane self-diffusivities in both pure and mixture are found to be larger than that of ethane. This is because methane is smaller than ethane.

Fig. 5 shows the center-of-mass distribution of the methane/ethane mixture in Zn(tbip) at different total concentration. It can be seen that at both, low and high concentrations the smaller and faster diffusing methane molecule, does not only easily diffuse from one leaf site to another leaf site in the same segment but also fastly diffuses through the ethane molecules and performs hops between the segments. Consequently, the self-diffusivity of methane is higher than that of ethane. The diffusion of ethane again shows a maximum at intermediate loadings. At highest loadings the steric hindrance effects cause a decrease for both methane and ethane diffusivity. In Fig. 5, we also observe that ethane molecules still prefer to locate in the center region of the channel and to adsorb closer to the windows more than in the case of CO_2/ethane mixtures.

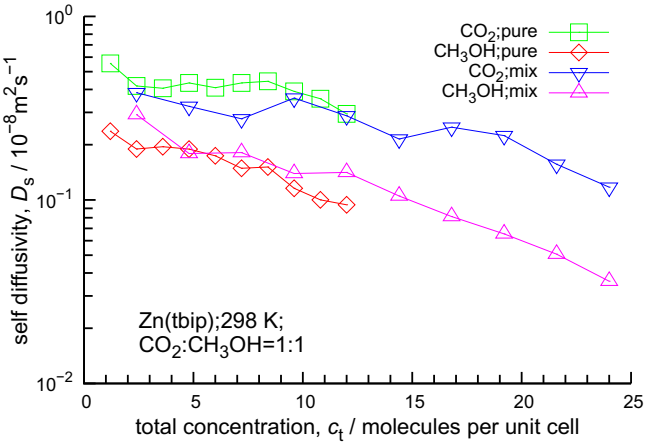

Fig. 7. The self-diffusivities of CO_2 and methanol both for pure components and 1:1 mixture in Zn(tbip) flexible framework.

3.3. CO_2/methanol mixture in Zn(tbip)

As we have mentioned above, CO_2 is a polar and more slender molecule than ethane, so that the surprising effect of the flexible lattice (maximum in the loading dependence) found for ethane is not to be expected and does not appear for CO_2. This behavior caused us to extend the investigation of Zn(tbip) with flexible lattice to methanol as guest molecule, which is also a polar molecule but has stronger confinement than CO_2, and mixtures of CO_2 and methanol. In Fig. 6 it can be seen that the lattice flexibility affects the self-diffusivity of methanol while that of CO_2 is nearly unaffected by the flexibility.

Fig. 7 shows the self-diffusivity of CO_2 and methanol, in both the pure and the mixture studies, as a function of total concentration. The CO_2 self-diffusivity is higher than that of methanol for the entire range of total concentrations. The density dependence shows the expected behavior discussed above for all mixtures.

Fig. 8 shows the center-of-mass distribution of CO_2 and methanol mixtures in Zn(tbip) at low and high total concentrations. It can be seen that methanol molecules prefer to be located at the leaf positions, and then preferably are adsorbed and sticking together

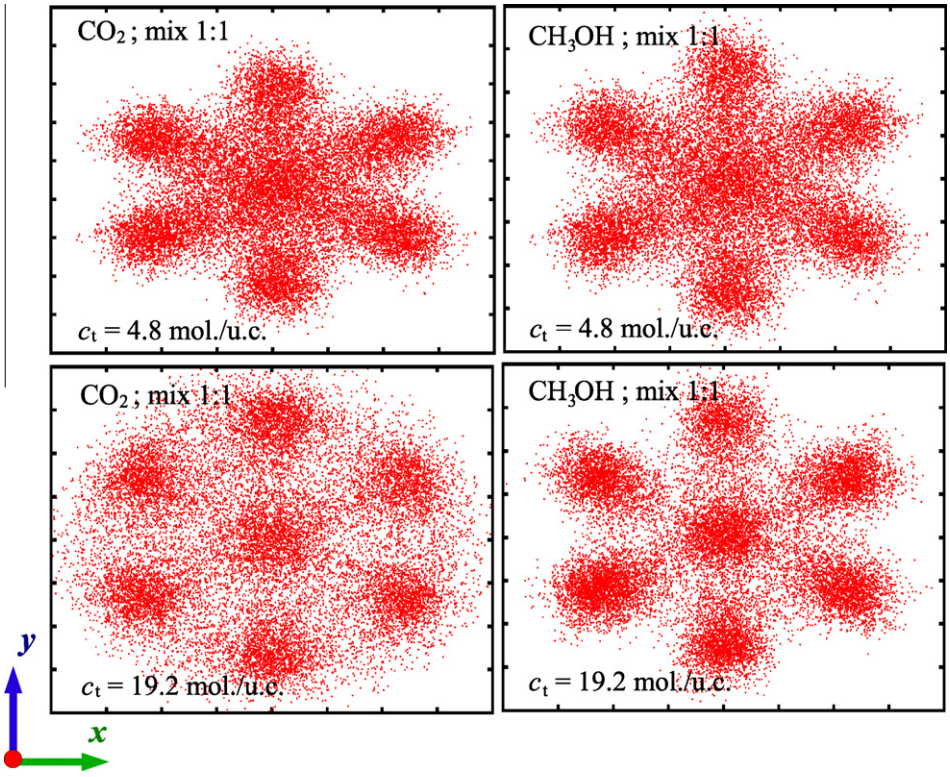

Fig. 8. The center-of-mass distribution of a CO_2 and methanol molecule projected into the *xy* plane tracked every 0.5 ps during a simulation period of 10 ns for CO_2:methanol = 1:1 mixture in Zn(tbip) flexible framework.

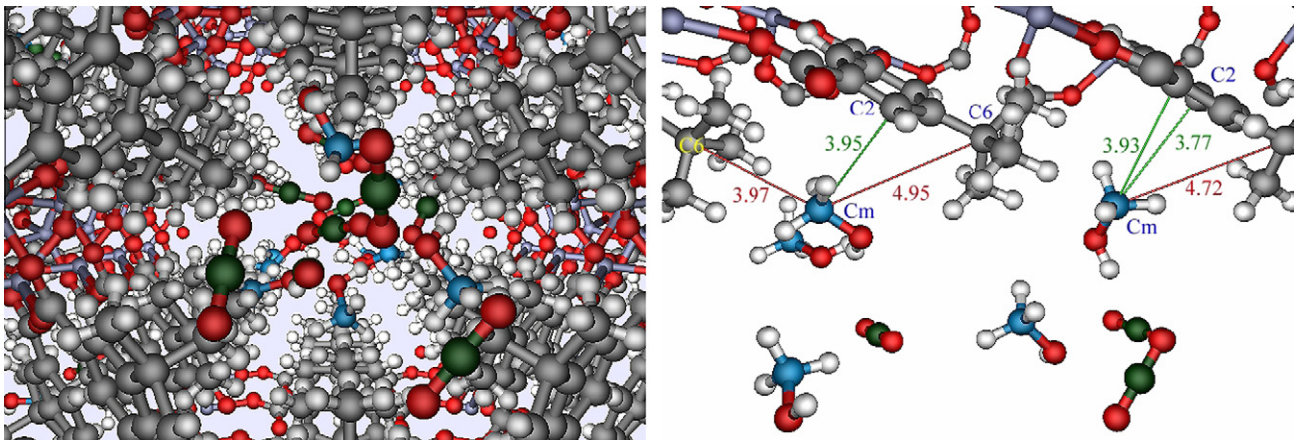

Fig. 9. The typical arrangement of CO_2 and methanol in a channel of Zn(tbip) at total concentration of 24 molecules per unit cell, also the typical C2—C_m and C6—C_m distance are presented in angstrom, giving values consistent with those observed the RDFs as shown in Fig. 10.

more and more when the loading increases. This behavior is also found in case of its pure components (not shown). This is a consequence of the electrostatic interactions between methanol molecules, as well as between methanol molecules and the framework. Because methanol prefers to be located at the leaf positions, the strong change of the framework at window regions found in the case of ethane, cannot be found in the case of methanol, as shown in Fig. 2. Hence, the methanol self-diffusivity does not show a maximum when the concentration is increased.

Because the CO_2 molecule is more slender than methanol the CO_2 self-diffusivity is larger than that of methanol for the full loading range studied. With increasing concentration both CO_2 and methanol self-diffusivities decrease monotonically.

3.4. Radial distribution functions

In addition, to gain insight into the typical locations and arrangements of methanol inside the segment of Zn(tbip) the RDFs of C2—C_m and C6—C_m have been evaluated. C2 represents the carbon atoms in the organic linker, or benzene groups, of Zn(tbip), C6 is the carbon atom that connects the methyl groups at the window, and C_m is the carbon atom of methanol, for each total concentration of the CO_2/methanol mixture in Zn(tbip) that has been evaluated. The results are given in Fig. 10. The C2—C_m RDF shows the typical first peak at about 4.00 Å, and about 4.75 Å for the C6—C_m. For both C2—C_m and C6—C_m the intensity of the first peak of $g(r)$ gradually increases with increasing mixture loading. These positions are consistent with the typical snapshots of the CO_2/ethanol mixture in Zn(tbip) that are shown in Fig. 9. These snapshots show that in the CO_2/methanol mixture in Zn(tbip), methanol molecules are preferentially adsorbed in the leaf positions of the framework. Simultaneously, the methanol

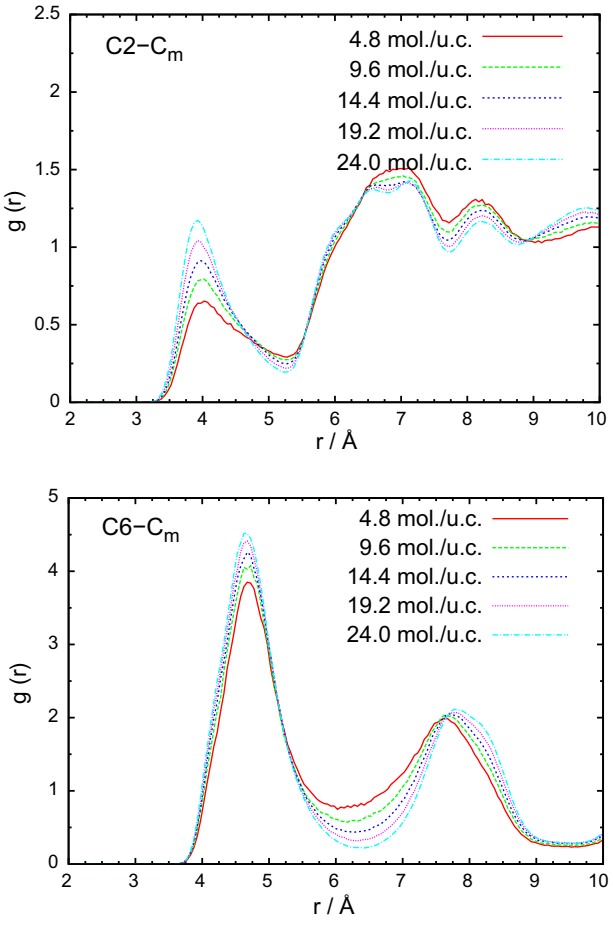

Fig. 10. The radial distribution function; g(r), for C2—C_m and C6—C_m, where C2, C6 are carbon atoms of Zn(tbip), see Fig. 9 for its coordinates, C_m is carbon atoms of methanol. The data are shown for different total concentrations of equimolar CO_2/methanol mixture in Zn(tbip) flexible framework.

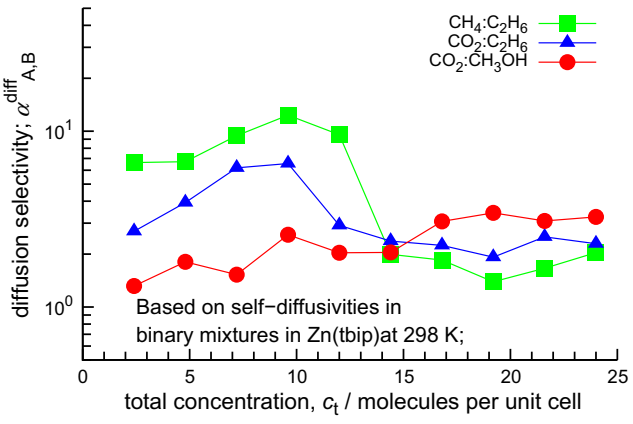

Fig. 11. The diffusion selectivities of methane/ethane, CO_2/ethane and CO_2/methanol mixtures in Zn(tbip) flexible framework.

molecules try to turn their axis perpendicular to the benzene ring of the framework, and to put the methyl group close to this ring.

3.5. Self-diffusion selectivity

The diffusion selectivities for the CO_2/ethane, the methane/ethane and the CO_2/methanol mixtures within Zn(tbip) with flexible framework were calculated using Eq. (4), as shown in Fig. 11. The $\alpha^{diff}_{CO_2,C_2H_6}$ values are in the range of 2–6 for the total concentrations; $c_t < 12$ molecules per unit cell, and then $\alpha^{diff}_{CO_2,C_2H_6}$ decreases when the total concentration is increased. This behavior indicates that for the CO_2/ethane mixture, diffusion is strongly selective at low loading where in average each segment of the framework is occupied by less than one ethane molecule. In the case of methane/ethane mixtures, the $\alpha^{diff}_{CH_4,C_2H_6}$ values are in the range of 6–12 and have the same trend as $\alpha^{diff}_{CO_2,C_2H_6}$ at low loading. In the case of CO_2/methanol mixtures, it can be seen that the $\alpha^{diff}_{CO_2,CH_3OH}$ values gradually increase with increasing concentration in the range of 1.0–3.5 for the range of studied concentrations, indicating that the diffusion is selective for CO_2 over methanol, especially at high concentrations.

4. Conclusions

In this work, molecular dynamics simulations have been used to investigate diffusion of three equimolar binary mixtures of CO_2/ethane, methane/ethane and CO_2/methanol, as well as pure component diffusion of methane, CO_2, methanol and ethane molecules. The results showed that the maximum in the self-diffusivity of ethane as a function of loading that was shown to be present only in the flexible lattice appears also in the mixture. The reasons for this maximum have been explained in [5]. Hence, the simulations of some technically important mixtures containing ethane in Zn(tbip) presented in this paper had clearly to be done in the flexible lattice. Moreover, additional simulations of pure CO_2 and methanol show that for methanol there is also non-negligible influence of the lattice flexibility.

Methane is a more compact molecule than ethane, thus the methane self-diffusivities are larger than for ethane. With increasing concentration, methane molecules are preferably located in the leaf site. And therefore the methane self-diffusivity decreases only monotonically.

CO_2 is a polar and more slender molecule than ethane, thus the CO_2 self-diffusivities are larger than for ethane. An increase in the CO_2 self-diffusivity is not observed.

Methanol is also a polar molecule with a slightly smaller molecular size compared to ethane, thus the methanol self-diffusivities are larger than for ethane. When the concentration increases, methanol molecules are preferably adsorbed and sticking together at the leaf sites, and therefore an increase in its self-diffusivity is also not observed.

In mixtures, the self-diffusivities of all diffusing molecules calculated at different total concentrations show that the faster diffusing molecules accelerate the slower diffusing molecules whereas, in turn, the slower molecules act to slow down the faster molecules through the channel of Zn(tbip) framework.

The diffusion selectivities for methane/ethane, CO_2/ethane and CO_2/methanol give values in the range of 1–12, but they show different trends.

For methane/ethane and CO_2/ethane mixtures, the diffusion selectivities have high values at seemingly low loadings, but high value were found at high loadings in the case CO_2/methanol mixture. This is indicating that Zn(tbip) may be a useful material for separating methane/ethane and CO_2/ethane mixtures at low concentrations, and CO_2/methanol mixtures at high concentrations.

Acknowledgement

S. Fritzsche and C. Chmelik gratefully acknowledge financial support from the DFG, SPP 1362. K. Seehamart thanks the Rajamangala University of Technology Isan (RMUTI) for a Ph.D. Grant. We thank J. Kärger (University of Leipzig), T. Nanok (Kasetsart University, Bangkok) and T. Remsungnen (Khon Kaen University) for interesting discussions about the content of this work. We thank the computer center of the university Leipzig and the center for information services and high performance computing (ZIH) of Dresden University of Technology for computer facilities and CPU time. R. Krishna acknowledges the DFG for the award of a Mercator Professorship.

References

[1] R. Krishna, J. Phys Chem. C. 113 (2009) 19756.
[2] R. Krishna, J.M. van Baten, Micropor. Mesopor. Mater. 137 (2011) 83.
[3] R. Krishna, J.M. van Baten, J. Phys. Chem. C 114 (2010) 18017.
[4] K. Seehamart, T. Nanok, R. Krishna, J.M. van Baten, R. Remsungnen, S. Fritzsche, Micropor. Mesopor. Mater. 125 (2009) 97.
[5] K. Seehamart, T. Nanok, J. Kaŕger, C. Chmelik, R. Krishna, S. Fritzsche, Micropor. Mesopor. Mater. 130 (2010) 92.
[6] D.C. Ford, D. Dubbeldam, R.Q. Snurr, Diffusion-fundamentals 11 (2009) 78. pp. 1–8.
[7] R. Krishna, J.M. van Baten, E. García-Pérez, S. Calero, Chem. Phys. Lett. 426 (2006) 219.
[8] R. Krishna, J.M. van Baten, Chem. Eng. J. 133 (2007) 121.
[9] M. Martin, J. Siepmann, J. Phys. Chem. B 102 (1998) 2569.
[10] R. Krishna, J.M. van Baten, Chem. Eng. Sci. 64 (2009) 3159.
[11] A.I. Skoulidas, D.S. Sholl, J. Phys. Chem. B 109 (2005) 15760.
[12] G. Garberoglio, R. Vallauri, Micropor. Mesopor. Mater. 116 (2008) 540.
[13] F. Stallmach, S. Gröger, V. Künzel, J. Kärger, O.M. Yaghi, M. Hesse, U. Müller, Angew. Chem. Int. Ed. 45 (2006) 2123.
[14] D.F. Plant, G. Maurin, R.G. Bell, J. Phys. Chem. B 111 (2007) 2836.
[15] D.F. Plant, G. Maurin, R.G. Bell, J. Phys. Chem. B 110 (2006) 15926.
[16] T. Nanok, S. Vasenkov, F.J. Keil, S. Fritzsch, Micropor. Mesopor. Mater. 127 (2010) 176.
[17] W. Smith, T. Forester, I. Todorov, M. Leslie, THE DL_POLY_2 USER MANUAL, CCLRC Daresbury Laboratory, UK, 2006.
[18] J.M. Haile, Molecular Dynamics Simulation: Elementary Method, John Wiley & Sons Inc., Clemson, SC, 1992.
[19] Q. Yang, C. Zhong, J. Phys. Chem. B 110 (2006) 17776.
[20] J. Liu, J.K. Johnson, J. Low. Temp. Phys. 175 (2009) 268.
[21] S. Keskin, J. Phys. Chem. C 114 (2010) 13047.